Oil Spill Detection by means of Neural Networks Algorithms: a Sensitivity Analysis

Fabio Del Frate, Luca Salvatori
Dipartimento di Informatica Sistemi e Produzione.
Tor Vergata University
Via del Politecnico, 1 I-00133 Rome, Italy
Tel: +39 06 72597421, Fax +39 06 72597460
delfrate@disp.uniroma2.it, salvatori@disp.uniroma2.it

***Abstract*— Synthetic Aperture Radar (SAR) images provided by satellite missions may provide a significant support for oil spill detection over the sea. In particular neural networks algorithms have recently demonstrated their potentialities for discrimination between oil spills and objects which resemble oil spills (called "look-alikes"). The main steps of the classification procedure are the identification of dark spots over the sea, the computing of a set of parameters (features) for each dark spot and the classification of the oil spill candidate using a trained neural network, where the network input is a vector containing the values of the features extracted. The features so far mainly consist of physical-geometrical characteristics of the dark spot. In this study we present a new neural network algorithm for the oil spill detection. The results also report a sensitivity analysis of the classification performance on the quantities that are given as input to the neural network. Among the considered inputs the value of the local wind speed has been also included.**

Keywords- synthetic aperture radar (SAR); neural networks; oil spill detection; CMOD4.

I. INTRODUCTION

Oil spills over the sea surface pollute the marine environment to a varying degree during large oil tanker accidents, especially when they occur close to the coast. But these accidents only account for a little percentage of total oil pollution worldwide, which is mainly due to wild discharges as oil releases from ships in transit when cleaning tanks. Satellite Synthetic Aperture Radar (SAR) images have proved to be suitable tools for identification of oil spills in the ocean. The radar backscattering cross section from clean water surfaces at incidence angles between 25 and 60 degrees can be described by Bragg scattering theory. According to this the sea clutter is mainly due to the short gravity and the gravity–capillary waves (from one centimetre to decimetres). The presence of an oil film on the sea surface damps these kinds of waves because of the resonance-type behaviour of the viscous-elastic surface films described by the Marangoni damping theory [1], [2]. So the presence of an oil film on the sea surface drastically reduces the measured backscattering energy, resulting in darker areas in SAR imagery. However, careful image analysis is required because dark areas might also be caused by locally low winds or by natural sea slicks, as shown in Figure 1 where different simultaneous events, which may cause low backscattering, are visible. Previous studies [3,4] reported on how automatic algorithms may be useful in supporting the decision-making process. They can operate either in a real-time mode, to assist watching and operation activities, or in batch mode, to retrieve statistics about oil spills events over a particular area or a period of time. In particular the effectiveness of a neural network approach for discriminating between real oil spill and look-alikes was already demonstrated in [3].

In this paper we report new results obtained by adding in the network input vector the wind speed information and investigating on the information content associated to each of its components.

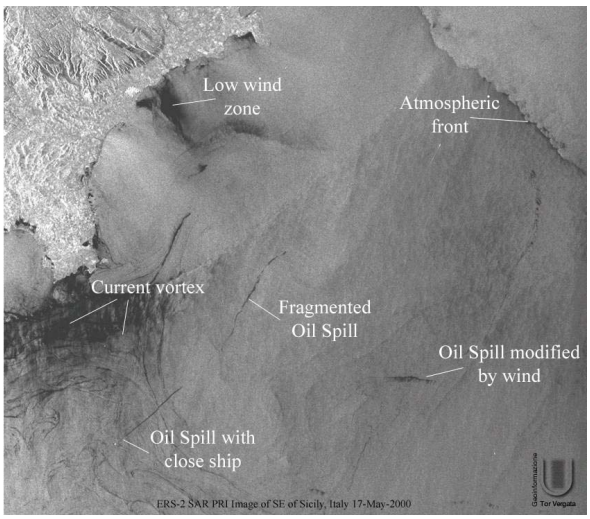

Figure 1. Different simultaneous events which may cause a reduction of the measured backsacttering energy.

II. THE ALGORITHM FOR THE OIL SPILL DETECTION

The neural scheme used in this study resembles the one already described in [3]. A semi-automatic tool allows the extraction of some salient features which characterize the selected dark spot in the image and that will be included in the neural network input vector. The features can be of three different types. Some of them contain information on the backscattering intensity (calculated in dB) gradient along the border of the analysed dark spot: *Max Gradient (Gmax), Mean Gradient (Gme), Gradient Standard Deviation (GSd)*; others focus on the backscattering in the dark spot and/or in the background: *Object Standard Deviation (OSd)*, *Background Standard Deviation (BSd)*, *Max Contrast (ConMax)*, *Mean Contrast (ConMe);* a third category takes into account the geometry and the shape of the dark spot: *Area (A), Perimeter (P)*, shape *Complexity (C), Spreading (S)* with respect to a longitudinal axis. More precise definitions can be found in [3].

In this work we considered an additional feature containing information on the local wind speed. The knowledge of the local wind vector is indeed important because it is the responsible of the short gravity and the gravity–capillary waves, so the wind speed can strongly influence the appearance of the oil slick in a SAR image. In particular, for wind speed less than 2-3 m/s dark areas due only to the lack of wind may be visible. For wind speed greater than 7-8 m/s but less than 15 m/s natural slicks are dispersed whereas oil slicks remain still connected. For wind speed greater than 15 m/s it is possible to have emulsion between water and oil so that the oil slicks become invisible to the SAR. The *Wind Speed (WS)* is calculated by means of the inversion of the CMOD4 model, an empirical model used by ESA to retrieve wind vectors from ERS C-band scatterometer measurements [5].

The CMOD4 model provides σ_0 values as a function of relative wind direction, φ, (φ=0 for a wind blowing towards the radar), wind speed and incidence angle, expressed as:

$$\sigma_0 = B_0[1 + B_1 \cos(\varphi) + B_3 \tanh(B_2)\cos(2\varphi)]^{1.6} \quad (1)$$

where the coefficients B_0, B_1, B_2 and B_3 depend on the local incidence angle of the radar beam and on the wind speed. The dependency of σ_0 on the different inputs is shown in Figure 2.

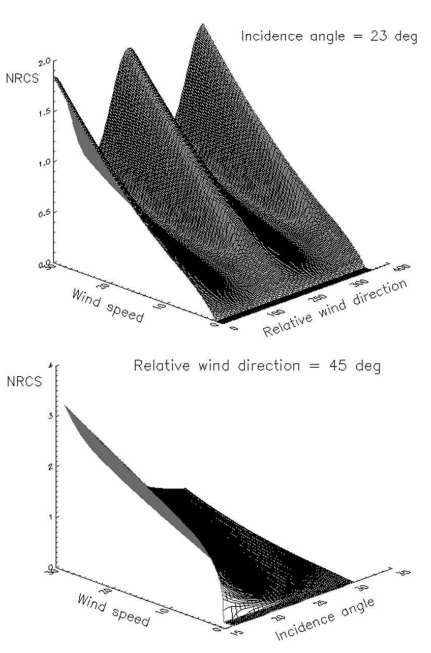

Figure 2. Dependence of Radar Cross Section on wind speed vector according to CMOD4 model.

One can see the periodic dependency on the relative wind direction, but the most important observation for the purpose of this paper is the monotone growing dependency on the wind speed that allows the inversion of the model [6]. Since the model relates the backscattering coefficient to wind speed, wind direction and incidence angle, to derive wind speed from a SAR image an estimate of the wind direction is required. To this end it is possible to use external information or the visual inspection. The wind speed estimations have been successfully validated with the information provided by the NASA wind-scatterometer QUIKSCAT.

III. THE NEURAL NETWORK

Starting from an archive of about 70 ERS-SAR images mainly taken over Mediterranean basin in the time period between 1996 and 2003 we extracted 189 dark objects, 111 oil spills and 78 look-alikes. For a number of examples ground-truth was available, else the discrimination was based on the independent judgment of experienced image analysts. The main statistical parameters describing the features extracted from the data set are shown in Table 1.

TABLE I. MAIN STATISTCAL PARAMETERS IN THE DATA SET.

Feature	Oil Spill				Look Alike			
	Max	Min	Mean	St.D.	Max	Min	Mean	St.D.
A (Km^2)	32.9	0.3	4.4	5.8	146.3	0.4	14.9	23.8
P(Km)	142.9	2.3	23.2	25.7	304	4.2	47.2	54.6
C	7	0.9	2.9	1.4	7.5	1.2	3.5	1.4
S	36	0	6.6	7.8	39	0	11.8	10.6
Osd(dB)	4.5	0.7	1.9	0.7	4.8	0.6	2.4	0.9
BSd(dB)	1.9	0.6	0.9	0.2	4.1	0.8	1.6	0.5
ConMax(dB)	17.8	4.2	9.5	3	18.5	4.7	12.4	2.8
ConMe(dB)	12.7	1.6	4.7	2	11.9	1.5	6.5	2.2
GMax(dB)	15.1	3.2	7.4	2.5	15.4	3.9	9	2.8
Gme(dB)	7.4	1.4	2.9	1.1	6.3	1.2	3.2	1.1
GSd(dB)	3	0.6	1.4	0.5	3	0.6	1.7	0.6
WS(m/s)	7.1	2	3.5	0.7	10.2	1.6	3	1.3

Several attempts have been initially made to properly select the number of units to be considered in the hidden layer of the neural network. The topology 12-8-8-1 (see Figure 3) has been finally chosen for its good performances both in terms of classification accuracy and of training time.

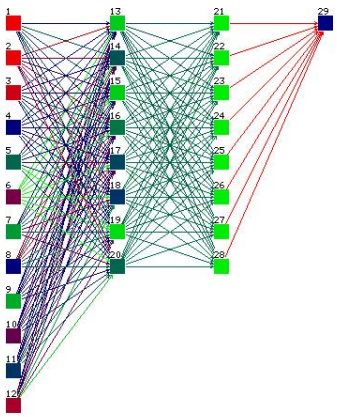

Figure 3. Topology of the neural network utilized.

The neural network has been trained to return 1 if a dark spot in the image is an oil spill, 0 if it is a look-alike. For determining when the training procedure had to be stopped

we considered the "early stopping" algorithm [7]. According to this algorithm, the performance of the net during the training (learning) phase is evaluated either on the training set or on a different independent validation set. In the training set the overall error in the retrieval of the correct output keeps on decreasing with the training, approaching a value of convergence. Conversely, the error on the validation set reaches a minimum value after which it will start increasing if we continue the training. At this point the learning phase must be interrupted. The dependence of the error on the number of epochs (training cycles) for the training and the validation set is shown in Figure 4.

The software simulations were performed by means of the Stuttgart neural network simulator (SNNS), developed at the University of Stuttgart (Germany) [8], which proved to be a high-level, flexible and reliable software package.

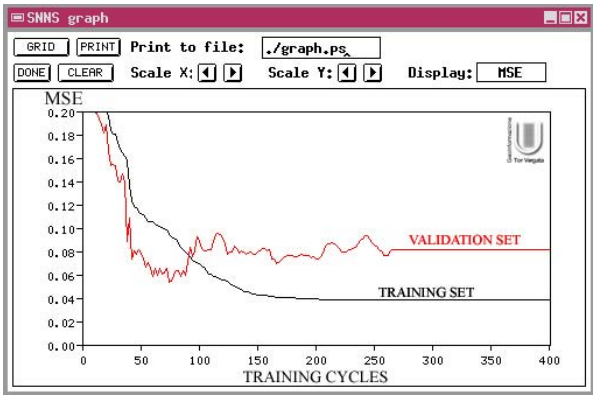

Figure 4. Dependence on the number of training cycles of the error for the training and the validation set .

The whole set of examples has been then divided in two sub-sets: a training set of 129 examples and a test set of 60 examples. After the training based on the learning set and applying the "early stopping" algorithm we found a root mean square error (rmse) of 0.227 on the test set (3 misclassified examples out of 60).

An optimization of the number of the connections characterizing the net has been also carried out, at this point, by using a pruning procedure. According to this procedure, a network is examined to assess the relative importance of its weights, and the less important ones are deleted by using the magnitude of a weight value as a measure of its importance. Typically this is followed by further training of the pruned network. By means of this procedure it is possible to simplify the topology of the neural network and concurrently improve its classification accuracy. For example, in our case, we continued the pruning procedure until we reached a minimum in the rmse value of 0.223, slightly better than with the net before the pruning.

IV. THE SENSITIVITY ANALYSIS

As discussed in [3] the reliability of the values for the features calculated by the semi-automatic tool depends on the ability of the user of managing the embedded edge detection utilities. In the perspective of a fully automatic tool it is then reasonable to suppose that he *S/N* ratio characterizing the values of the features may significantly decrease. In this case a selection of the inputs to the network, on the base of the effectiveness of their information content in estimating the output, might be recommended to eliminate unnecessary or misleading inputs. A network with fewer inputs has fewer adaptive parameters to be determined, which need a smaller training set to be properly constrained. This leads to a network with improved generalization properties providing smoother mappings. In addition, a network with fewer weights may be faster to train.

In the attempt to examine which features, in the chosen context, contain less information for the classification task we considered two methods. In a first analysis we evaluated the network performance, both in terms of the rmse and of the misclassification rate, for 12 different cases where, on turn, one of the components of the initially considered input configuration was missing. In a second analysis we prolonged the pruning procedure (described before) to the input layer, until 11 of the 12 components of the input vector were removed (we remind that an input or hidden unit is removed when it has lost all its connections).

From the first methodology we observed that each of the considered 12 cases provokes a decrease of the classification accuracy with respect to the initial configuration with 12 inputs. This confirms a rather important property of neural networks, that is its ability to constructively use the different pieces of information associated to the calculated features. In most cases, the worsening of the performance does not exceed the value of 10% in terms of rmse and is around the same value of percentage in terms of misclassification rate. The most significant exception is represented by the feature BSd. Not considering it in the network input vector dramatically degrades the performance of the algorithm: we have for the rmse a value of 0.398 (increase of about 75% with respect to initial configuration) and a misclassification rate of 13 examples out of 60 (increase of about 433%). The meaningfulness of such a feature can be explained looking at the statistics reported in Table 1. We see that for both classes (oil spill and look-alike) the standard deviation values of the features are rather low and, on the other hand, their mean values (0.9 and 1.6, respectively) allow good level of separability. The only other features that, after BSd, provoke a rather significant degrade in the classification are GSd and OSd. Indeed without GSd we have an increase of 7.47% in the rmse and an increase of 33.33% in the misclassification rate, whereas without the OSd an increase of 5.92% in the rmse and an increase of 33.33% in the misclassification rate. A further general comment should focus on the fact that, collectively, physical features, in particular those indicating standard deviation values, seem to be more significant then geometrical features.

The results obtained in the second analysis, with the extended pruning procedure, are in good agreement with those commented above. BSd feature is the last one to be removed during the input units elimination process. In a rating of the channels deduced from the order of removal of the input units the first four standings are, in order, occupied by BSd, WS, GSd and OSd. Therefore also the information content brought in by wind speed is shown to be important in this case. This result is in accordance to the fact that, as it was illustrated before, the general conditions of the sea surface surrounding the slicks affect the actual capability of the SAR to detect the slicks.

V. TOWARDS AUTOMATIC PROCEDURES

The latter kind of analysis has been done to the aim of optimizing the design of a fully automatic version of the oil spill detection algorithm, currently under development. A fully automatic procedure involves a loss in terms of accuracy, above all for the impossibility of supervising the correct extraction of the dark spots. This motivates the efforts to concentrate the processing towards the most significant image parameters. On the other hand, this loss of accuracy is well acceptable considering the importance of an automatic algorithm for oil spill detection. This would allow the set-up of procedures which can work autonomously and continuously, elaborating large archives of images and, providing preliminary classification, reducing the time for visual inspection usually required to human operators. It has also to be observed that the construction of an automatic procedure involves facing with other problems such as land masking, which in our case was solved on the base of external geographic information.

VI. CONCLUSIONS

This study follows the work described in [3] where the potentialities of neural network algorithms for the detection of oil spills in satellite SAR imagery have been demonstrated. A procedure to calculate the local wind speed directly from a SAR image has been developed in order to use this information as additional input for the neural network and to know the evolution of the oil spills. The neural network obtained after the training phase has been able to correctly discriminate over a set of independent examples between oil spills and look-alikes with a largely acceptable rate of success. The relative importance of the features included in the input vector has been estimated with two sensitivity analysis techniques. They pointed out the importance of some physical parameters (such as the standard deviation of the backscattering intensity values of the pixels belonging the sea surface surrounding the analyzed dark spot, BSd, or the standard deviation of the backscattering intensity gradient values of the pixels along the border of the dark spot, GSd) and that, in general, the information content of physical parameters seems to be larger than the one of geometrical and shape parameters. The possibility of making completely automatic the oil spill detection has also been explored, and it is still object of study. The performance, in this case, mainly depends on a correct extraction of the dark object, and the most part of the efforts should be addressed to this problem. The methodologies described in this paper have been implemented in software tools, developed in IDL language. The outputs provided by these software are geo-referenced and GIS compatible, to allow their use in common GIS environments. It must be noted that the designed procedure can easily process both ERS and ENVISAT imagery.

ACKNOWLEDGEMENT

The work carried out in this study has been done also thanks to the support and the experience of Dr. Juerg Lichtnegger.

REFERENCES

[1] W. Alpers, and H.Huhnerfuss, "Radar signatures of oil films floating on the sea surface and the Marangoni effect", Journal of Geophysical Research, vol.93, pp.3642--3648, 1988.

[2] W. Alpers, and H.Huhnerfuss, "The damping of ocean waves by surface films: a new look at an old problem", Journal of Geophysical Research, vol.94, pp.6251--6265, 1989.

[3] F. Del Frate, A. Petrocchi, J. Lichtenegger, G. Calabresi, "Neural networks for oil spill detection using ERS-SAR data", IEEE Trans. Geoscience and Remote Sensing, Vol.38, No.5, pp. 2282—2287, 2000.

[4] A. H. Schistad Solberg, G. Storvik, R. Solberg, E. Volden "Automatic Detection of Oil Spills in ERS SAR Images", IEEE Trans. Geoscience and Remote Sensing, Vol.37, No.4, pp. 1916—1924, 1999.

[5] P. Lecomte, "*CMOD4 Model Description"*, ESA-ESRIN.

[6] F. Del Frate, L. Salvatori, J. Lichtenegger, A. Petrocchi**,** "Sea Pollution Monitoring with Neural Networks and Satellite Data", proceedings of "2003 Tyrrhenian International Workshop on Remote Sensing", pag.649-656, 2003.

[7] C. M. Bishop, "*Neural Networks for Pattern Recognition"*, Oxford Univ. Press, pp. 374--375, 1995.

[8] A. Zell, et al., "*SNNS Stuttgart Neural Network Simulator User Manual"*, Report N6/95, University of Stuttgart, Institute for Parallel and Distributed High Performance Systems, Stuttgart, Germany, 1995.